The Journal of Eukaryotic Microbiology

ISOP Published by the International Society of Protistologists

Journal of Eukaryotic Microbiology ISSN 1066-5234

ORIGINAL ARTICLE

Nuclear Features of the Heterotrich Ciliate *Blepharisma americanum*: Genomic Amplification, Life Cycle, and Nuclear Inclusion

Megan M. Wancura[a], Ying Yan[a,b], Laura A. Katz[a,c] & Xyrus X. Maurer-Alcalá[a,c]

a Department of Biological Sciences, Smith College, Northampton, Massachusetts 01063, USA
b Institute of Evolution & Marine Biodiversity, Ocean University of China, Qingdao 266003, China
c Program in Organismic and Evolutionary Biology, University of Massachusetts Amherst, Amherst, Massachusetts 01003, USA

Keywords
Confocal; fluorescence; genome amplification; nucleus.

Correspondence
X.X. Maurer-Alcalá, Program in Organismic and Evolutionary Biology, University of Massachusetts Amherst, Amherst, MA 01003, USA
Telephone number: +1 413-585-3750;
FAX number: +1 413-585-3786;
e-mail: xmaurera@cns.umass.edu

Received: 8 August 2016; revised 10 April 2017; accepted April 12, 2017.
Early View publication June 7, 2017

doi:10.1111/jeu.12422

ABSTRACT

Blepharisma americanum, a member of the understudied ciliate class Heterotrichea, has a moniliform somatic macronucleus that resembles beads on a string. *Blepharisma americanum* is distinguishable by its pink coloration derived from the autofluorescent pigment blepharismin and tends to have a single somatic macronucleus with 3–6 nodes and multiple germline micronuclei. We used fluorescence confocal microscopy to explore the DNA content and amplification between the somatic and germline nuclei of *B. americanum* through its life cycle. We estimate that the DNA content of the macronucleus and micronucleus are 43 ± 8 Gbp and 83 ± 16 Mbp respectively. This correlates with an approximate DNA content difference of 500-fold from micronucleus to macronucleus and a macronuclear ploidy of ~1,100 N as compared to the presumably diploid micronucleus. We also investigate a previously reported macronuclear inclusion, which is present sporadically across all life cycle stages; this inclusion looks as if it contains blepharismin based on its fluorescent properties, but its function remains unknown. We also provide additional detail to our understanding of life cycles changes in *B. americanum* by analyses of fluorescent images. Overall, the data analyzed here contribute to our understanding of the diversity of nuclear architecture in ciliates by providing details on the highly polyploid somatic macronucleus of *B. americanum*.

CILIATES are unicellular organisms characterized by the presence of cilia and nuclear dualism (i.e. they have both a somatic macronucleus and a germline micronucleus within each cell/organism). The macronucleus is responsible for most cellular activity, while the micronucleus is quiescent throughout most of the life cycle. During conjugation, meiotic products of micronuclei are exchanged and fused, forming a new zygotic micronucleus that then divides mitotically (McGrath et al. 2007; Prescott 1994). One of these nuclei then undergoes extensive processing (including DNA elimination, chromosome fragmentation, and amplification) resulting in a newly developed macronucleus (McGrath et al. 2007; Prescott 1994).

Most ciliates have polyploid macronuclei, but the level of ploidy varies greatly among the classes studied to date. The macronuclei of some ciliates such as *Tetrahymena thermophila* (Cl: Oligohymenophorea) have a roughly equal ploidy of 45N (Raikov 1996; Turkewitz et al. 2002) while ciliates in the classes Armophorea, Phyllopharyngea, and Spirotrichea have "gene-sized" chromosomes that are independently amplified and can be present in thousands of copies (Huang and Katz 2014; Xu et al. 2012). The class Heterotrichea, the focus of this study, has been the subject of numerous morphological studies, yet few focus on the structure of their nuclei (e.g. Guttes and Guttes 1960; Kovaleva et al. 1997a,b; Ovchinnikova et al. 1965).

We analyze the macronuclear and micronuclear genome content of *Blepharisma americanum* (Cl: Heterotrichea), and then describe changes in macronuclear morphology throughout the life cycle. *Blepharisma* is marked by pink coloration due to the presence of the photosensitizing pigment blepharismin (Giese 1973). Additional unusual features of the genus *Blepharisma* include cannibalism, a phenomenon that allows the organism to grow giant

(McLoughlin 1957; Young 1938) and multiconjugation, by which sets of three, or, more rarely up to five organisms mate (Giese 1973; Weisz 1950). The macronucleus of *B. americanum* is described as moniliform, resembling "beads-on-a-string" (Giese 1973; Suzuki 1954). This species is also reported to have a "nuclear inclusion" in its macronucleus, though the chemical identity and function of this inclusion is unknown (Kennedy 1965; Young 1938).

Previous investigations of the nuclear morphology of *Blepharisma* species were done in an era before modern microscopy techniques (Giese 1973; Kennedy 1965; McLoughlin 1957; Suzuki 1954; Young 1938). With the exception of the examination of *Blepharisma undulans* Stein using TEM (Kennedy 1965), observations have been collected using nuclear stains with light microscopy and results reported with drawings, demonstrating the variable nature of *B. americanum* in both cell size and changes in macronuclear morphology throughout its life cycle (Giese 1973; Kennedy 1965; McLoughlin 1957; Suzuki 1954; Young 1938). Fluorescent microscopy, the approach used here, allows for detailed observations of nuclear morphology throughout ciliate life cycles (Maurer-Alcalá and Katz 2016; Postberg et al. 2005), as well as estimates of ploidy levels.

Ploidy and genome content have been estimated in diverse eukaryotes with a variety of techniques (Cousin et al. 2009; Prescott 1994; Xu et al. 2012). Quantification of fluorescence from DAPI is one method that has been used to estimate genome sizes in diverse protists (LaJeunesse et al. 2005; Mukherjee et al. 2009; Parfrey and Katz 2010; Whittaker et al. 2012) as well as in plants where genome sizes between genera can span several orders of magnitude (e.g. 125 Mbp in *Arabidopsis thaliana* to 22 Gbp in *Pinus taeda*; Suda and Trávníček 2006; Kaul et al. 2000; Zimin et al. 2014). There are limitations when using fluorescence to estimate genomic features, including preferential binding by DAPI for A-T rich regions of chromosomes, which can lead to inaccurate estimations of the genome size (Doležel et al. 1992; Noirot et al. 2002). Despite this potential bias, estimates with DAPI still provide useful approximations of genome size, especially in organisms where few genomic/molecular data currently exist.

In this study, we use DAPI staining and confocal microscopy to investigate several features of *B. americanum* including: (i) its macronuclear morphology throughout life cycle stages (ii) the relative DNA amplification during macronuclear development and (iii) a nuclear inclusion in the somatic macronucleus. These data provide insights into the nuclear dynamics of *B. americanum* and highlight the need for further work in this understudied ciliate lineage.

MATERIALS AND METHODS

Culturing

Blepharisma americanum were obtained from Carolina Biological (131430) and cultured in either filtered pond water or *Blepharisma* culturing solution (Giese 1973). Cells were cultured in 6-well plates at room temperature with a rice grain to support bacterial growth. Cultures were renewed biweekly by moving a small number of *B. americanum* to a new well with fresh filtered pond water and a rice grain.

Fixation and DAPI staining

To prepare samples for fixation, concentrated cells were collected via pipette and placed in 1.5 ml-centrifuge tubes and then filled to 1 ml with pond water or culturing solution depending on culturing conditions. Cells were centrifuged at 1,000 *g* for 5 min and excess water was removed. *Allium cepa* root tips, *Saccharomyces cerevisiae*, and epithelial cells from human oral mucosa were also prepared for fixation. Cells were fixed with either 8% PFA/0.2% Triton-x100 in a 1:5 ratio, or 20% PFA/50% RNALater/5% Trizol in a 1:6 ratio, on Superfrost (Fisher, Waltham, MA) microscope slides for 15 min, and then were washed twice for 2 min with 1× PBS. Slides were incubated with DAPI (0.1 mg/ml; Fisher) in the dark for 5 min. Cells were then rinsed three times with 1× PBS. A drop of SlowFade Gold (Invitrogen, Carlsbad, CA) was added and slides were sealed with nail polish.

Imaging

Images were collected on a Leica TCS SP5 laser scanning confocal microscope (63× oil immersion objective). The UV laser with an excitation wavelength of 405 nm was used to visualize DAPI, the argon laser with an excitation wavelength of 488 nm was used to collect DIC images, and the 514 nm argon laser was used to collect red light from blepharismin. Images of the nuclear inclusion were captured with a resolution of 1,024 × 1,024, with an acquisition speed of 200 Hz, and line average of 7. *Z*-stacks of *A. cepa*, *S. cerevisiae*, *Homo sapiens*, and *B. americanum* nuclei for determination of DNA content were collected at 1,024 × 1,024, 400 Hz, with a line average of 5, and a *z*-step of 0.29 μm. For the macronuclear inclusion, *Z*-stacks were imaged with a *z*-step of 0.5 μm. All cells and their nuclei were selected for imaging so as to reduce artifacts introduced from their preparation (i.e. we focused on cells that retained their morphology).

Image quantification

Genome amplification

The fluorescence intensities and volumes for a total of 50 *S. cerevisiae* nuclei, 53 *H. sapiens* cheek nuclei, 38 *A. cepa* root tip nuclei, 24 *B. americanum* macronuclei, and 65 *B. americanum* micronuclei were used for analysis. *Z*-stack profiles were analyzed using ImageJ (Rasband, W.S. ImageJ. U. S. National Institutes of Health, Bethesda, MD, http://imagej.nih.gov/ij/, 1997–2014; Table S1). The macro 3D Objects Counter, was used to quantify the total fluorescence of the nuclei integrated across volume (Cordelieres, F. P. 3D Objects Counter; ImageJ).

Fluorescence data from *A. cepa, S. cerevisiae, H. sapiens* were used as standards as they have well-established genome sizes. These standards were used to assess the variability in the intensity of DAPI staining. Estimates of the relationship between each unit of fluorescence intensity (FI) and known genome size are 356 bp/FI for *S. cerevisiae*, 410 bp/FI for *H. sapiens*, and 522 bp/FI for *A. cepa* nuclei. To account for the variability in the relationship between fluorescence signal and genome size, we made three estimates of the DNA content for *B. americanum*: (i) an "average" estimate based on our three standards (429 bp/FI); (ii) a "maximum" calculated using *A. cepa value of* 522 bp/FI; and (iii) a "minimum" based on *S. cerevisiae* value of 356 bp/FI.

Nuclear inclusion

ImageJ transects were taken spanning the greatest diameter of the nuclear inclusion or the brightest area of fluorescence for blepharismin across 10 nm sections from 580 to 640 nm. Each set of measurements was averaged to get one value for each image at each point of emission and divided by the largest point to give comparable ratios.

RESULTS

Genomic amplification in *Blepharisma americanum*

Using fluorescence microscopy, we investigated the relative size and genome content of the macronucleus and micronucleus of *B. americanum*. Estimates for the average volume of *B. americanum*'s micronuclei and macronuclei are 11 μm^3 and 5,521 μm^3 respectively (Table 1 and Table S1; estimates were taken as the volume of fluorescence for each nucleus of the *Z*-stacks for each cell). Nuclear volume and fluorescent signal are strongly correlated ($R = 0.975$, $p \ll 0.05$; Fig. 1), allowing us to estimate DNA content from *B. americanum*.

We estimated the DNA content for *B. americanum*'s macronucleus and micronuclei using the average fluorescence of the three "standards"—yeast (*S. cerevisiae*), human (*H. sapiens*), and onion (*A. cepa*)—that were chosen based on their range of genome sizes (Table 1 and Table S1) to determine the approximate relationship between fluorescence intensity and DNA content. Here, we report the minimum and maximum estimates of *Blepharisma*'s nuclear DNA content based on these standards. Using this approach, the somatic macronuclear DNA content is 43 ± 8 Gbp (min: 32 Gbp; max: 52 Gbp) whereas the germline micronuclear DNA content is 84 ± 16 Mbp (min: 69 Mbp; max: 101 Mbp; Table 1). We then estimated the relative ploidy difference between macronucleus and micronucleus based on the assumption that the micronucleus is likely diploid (Prescott 1994). This approach yields an approximate macronuclear ploidy of 1,027 N. This value represents a rough approximation, as it does not account for processing of DNA during macronuclear development, which includes elimination of noncoding DNA in other ciliates lineages (Allen and Nowacki 2017; Liu et al. 2005; McGrath et al. 2007; Prescott 1994).

Table 1. DNA content and genome size estimates from fluorescence emission of five types of nuclei

Nuclei	Avg. fluorescence	DNA content (Mbp)
Blepharisma americanum macronucleus	99,187,747	42,560 (32,270/51,789)
Blepharisma americanum micronucleus	193,231	82.9 (68.7/100.9)
Allium cepa	30,412,972	15,876
Homo sapiens	8,053,061	3,300
Saccharomyces cerevisiae	35,145	12.5

We estimated the genome sizes of *B. americanum* macronucleus and micronucleus using *A. cepa*, *H. sapiens*, and *S. cerevisiae* nuclei as standards.

Numbers in parentheses represent minimum and maximum estimates as discussed in Methods.

Life cycle

We assessed macronuclear morphology and arrangement in the various life cycle stages of *B. americanum*. Due to the inability to make synchronous cultures of *B. americanum*, we scanned mixed populations for cells in various stages (e.g. conjugation, actively dividing, and log-growth) and described patterns for each stage that we observed at least five times (Table 2). A total of 93 *B. americanum* imaged in this study produced images of suitable quality for further analyses. We excluded *B. americanum* cells that had clear irregularities in their membranes and/or disarrayed macronuclei (likely fixation artifacts). We observed three major forms of *B. americanum* macronuclei during cell division: (i) moniliform arrangement of macronuclear nodes (Fig. 2A, F), (ii) tight clustering of separated macronuclear nodes (Fig. 2C) and (iii) the elongation of the macronucleus associated with cell division (Fig. 2E). The largest proportion of somatic nuclei (53/93; 56.9%) appeared as the typical "beads-on-a-string" (moniliform) arrangement of macronuclear nodes with interspersed micronuclei present in highly variable numbers, often in close proximity to the macronucleus (Fig. 2A, F). For vegetative cells (e.g. cells that are neither dividing nor conjugating), there are on average four macronuclear nodes, most often ranging from three to six, with larger terminal nodes than interior nodes (Fig. 2A, F), although the number and size of these nodes is highly variable with some terminal nodes not being distinctly larger than any internal node.

During the onset of division (and presumably amitosis), the thin nuclear envelope connections between macronuclear nodes disappear and the nodes migrate together (12/93; 12.9%, Fig. 2B, C), eventually forming a large mass. Following this condensation of somatic nodes, the large macronuclear mass elongates into either very thick or thin strands, where the macronuclear nodes are underdeveloped, which we propose is toward the final step of amitosis and prior to cell division (18/93; 19.4%, Fig. 2D, E).

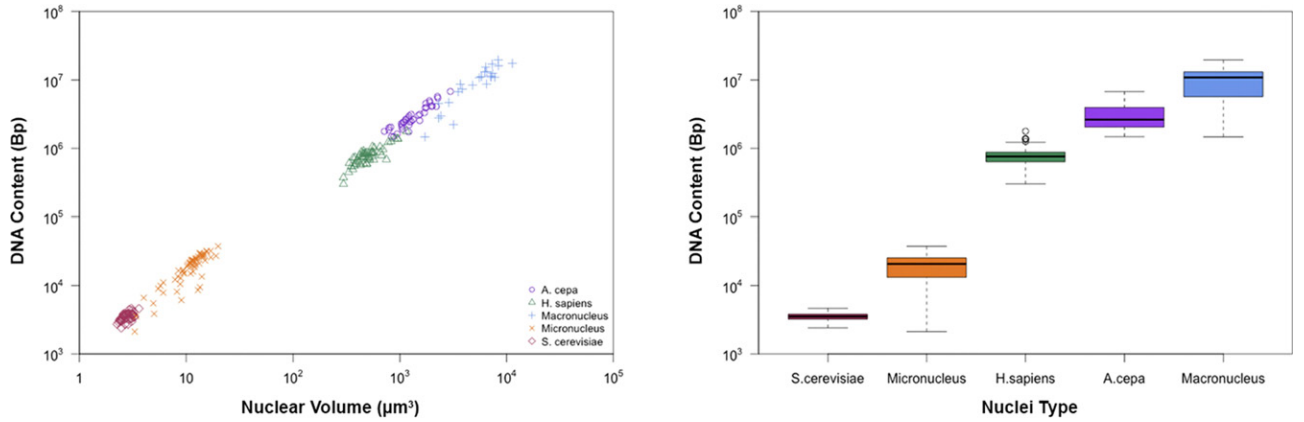

Figure 1 Left: This scatterplot shows the linear relationship of DNA content to the volume of nuclei. DNA content of *Blepharisma americanum* macronuclei is estimated to be 43 ± 8 Gbp and micronuclei is estimated to be 83 ± 16 Mbp. Right: Boxplot representing the total DNA content for the nuclei studied in this work: *Saccharomyces cerevisiae* (Yeast—Brown), *Blepharisma americanum* micronucleus (Orange), *Homo sapiens* (Human—Green), *Allium cepa* (Onion—Purple), and *B. americanum* macronucleus (Blue). Shaded regions represent the interquartile range, with the upper limit representing the third quartile and the lower limit representing the first quartile. Black lines through the middle of the shaded region represent median values. Lines drawn through the boxes extend to maximum and minimum values with unfilled circles representing suspected outliers.

Table 2. Nuclear inclusions present in nearly all life cycle stages in *Blepharisma americanum*

Cell life stage	No. of cells	Cells with nuclear inclusion
Vegetative	53	22
Amitosis	30	17
Conjugation	10	9

We did fix a small number of cells (10/93; 10.8%) during conjugation, as determined by the connection of two *B. americanum* across their oral apparatuses. However, we were unable to identify micronuclei undergoing mitosis for two potential reasons: (i) it is a brief event that occurs and the number of cells imaged was insufficient to observe their mitosis and (ii) their close proximity to the macronucleus makes it very difficult to distinguish changes in micronuclear morphology due to their relative small size.

Nuclear inclusion

Examination of the nuclear morphology of *B. americanum* led to several insights into the presence of a DNA-poor inclusion found in the macronuclei. Of the 93 life cycle images captured of *B. americanum*, 52 showed a small nuclear inclusion in one or more macronuclear nodes across all stages of life (52/93; 55.9%). Of the 18 nondividing macronuclei in the "beads on a string" formation showing the presence of nuclear inclusions (18/24; Table 2), 18 terminal nodes showed inclusions vs. 10 nonterminal nodes, indicating a predominance in their presence in terminal nodes. These inclusions are roughly spherical, as determined by Z-series scans (Fig. 3), and have an average diameter of 1.9 µm based on 60 inclusions in 32 individuals. About 79% of the macronuclear inclusions measured, when excited with a UV laser, emitted red light with spectra highly matching that of blepharismin (Fig. 4).

DISCUSSION

In this study, we estimate the DNA content of *B. americanum* macronuclei and micronuclei, propose three macronuclear configurations that vary across major life cycle stages, and present data on the macronuclear inclusion as analyzed by fluorescence confocal microscopy. We also demonstrate the utility of DAPI staining as a means of estimating DNA content and genome size in poorly studied lineages of eukaryotes.

Genome amplification

Based on the extreme size difference between *B. americanum*'s macronuclei and micronuclei, we predicted that macronuclei would contain far more DNA than micronuclei. The linear relationship between genome size and DAPI fluorescence presented in this study suggests that fluorescent microscopy is accurate enough to make preliminary estimates of genome sizes (Fig. 1). Using the correlation between fluorescence and known DNA content for our three standard eukaryotes (yeast, onion, and human), we estimate DNA content for the macronucleus (43 ± 8 Gbp; Table 1) and micronucleus of *B. americanum* (84 ± 16 Mbp; Table 1) and calculate that the macronuclear genome is approximately 1,000 times the amplification of the germline DNA. The level of amplification is probably an underestimate as some amount of the germline genome is likely to be eliminated during the development of the somatic genome of *B. americanum*. Among other ciliates, *T. thermophila* eliminates ~30% of its

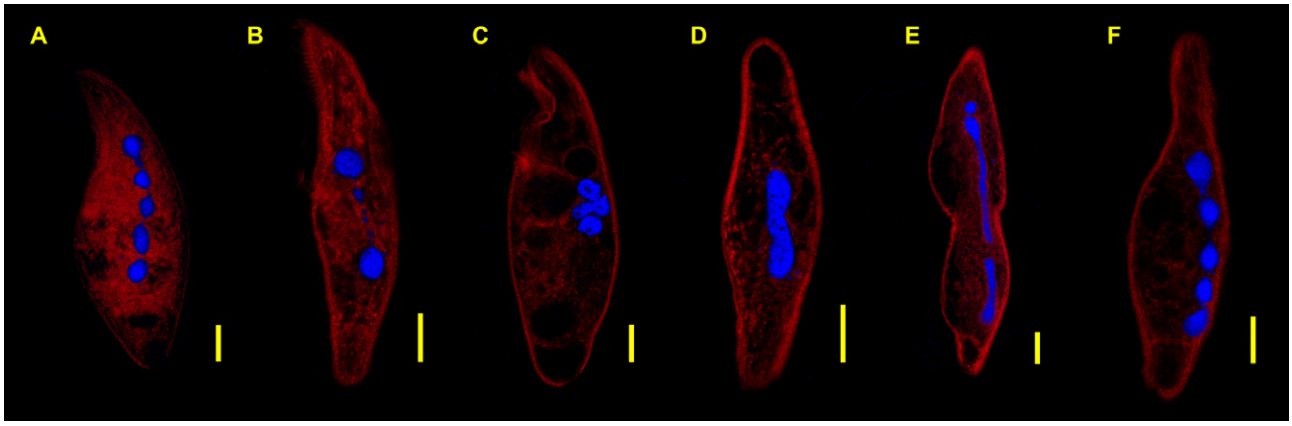

Figure 2 Morphological changes in the *Blepharisma americanum* macronucleus during amitosis. (**A**) Macronucleus with five distinct nodes in asexual growth. (**B**) Dissolution of connecting strands and migration of middle nodes. (**C**) Condensing macronuclear nodes. (**D**) Macronuclei extending into rod-like form. (**E**) Rod-like form pinching across middle and enlargement of terminal nodes. (**F**) Return to the nondividing macronuclear morphology. DNA (blue) and Blepharismin (red). Scale bar = 20 μm.

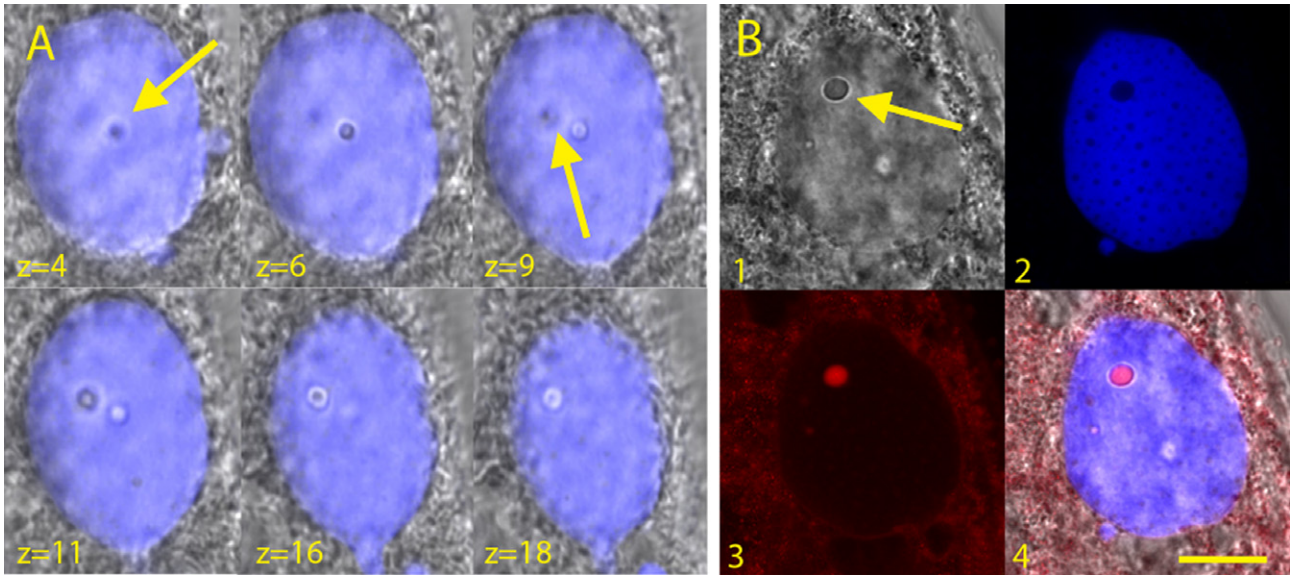

Figure 3 Macronuclear inclusion of *Blepharisma americanum*. (**A**) *Z*-series through the macronuclear inclusion, where each slice corresponds to 0.5 μm. (**B**) 1. DIC image of a macronuclear node. 2. DAPI staining. 3. Red emission. 4. Overlay of DIC, DAPI staining and red emission. Arrows indicate the location of the nuclear inclusion. Scale bar = 10 μm.

germline DNA sequences from the developing macronucleus (Liu et al. 2005; Yao and Gorovsky 1974), while *Chilodonella uncinata*, *Oxytricha trifallax* and *Stylonychia lemnae* eliminate from 35 to 95% of their germline sequences (Prescott 1994).

The relationship of nuclear size to fluorescence supports the insights by Cavalier-Smith (2005) that nuclear size is directly related to DNA content. Under this model, the large macronuclear volume of *B. americanum* may have evolved to support the relatively large cell size (~250–350 μm). This relationship holds across taxa as the yeast *S. cerevisiae* had the smallest nuclei by volume and much lower total fluorescence as compared to the larger nuclei of *A. cepa* and *B. americanum* (Fig. 1).

Life cycle

Changes in the morphology of the macronucleus throughout the life cycle of *B. americanum* proposed here are comparable to previously observed macronuclear behaviors (Giese 1973; Kennedy 1965; McLoughlin 1957; Suzuki 1954; Young 1938). During the dominant nondividing life cycle stage, *B. americanum*'s macronucleus is present as a set of nodes interconnected with a thin string of macronuclear DNA (Fig. 2A, F). The individuals in our study were found to have 3–6 macronuclear nodes, consistent with Giese's findings (1973), although other studies have indicated that the number of macronuclear nodes in *B. americanum* can range from 2 to 10 (Giese 1973;

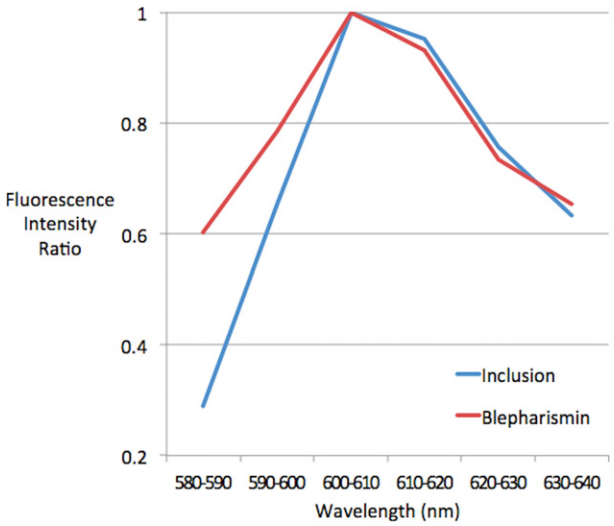

Figure 4 Comparative emission spectra for the macronuclear inclusion and blepharismin ($n = 15$ for blepharismin and $n = 14$ for macronuclear inclusion). Both spectra show a maximum emission at 600–610 nm and a similar shape.

Kennedy 1965; McLoughlin 1957). Suzuki (1954) observed that the terminal nodes of the macronucleus are always larger in size than the interior nodes although these differences in size are highly variable, which is again consistent with our observations.

Our analysis of cells in division is consistent with published work that describes amitosis in *B. americanum*. Initially, the thin strands between inner nodes disappear, and the inner nodes begin to congregate (Fig. 2B; Suzuki 1954; Young 1938; Weisz 1949). This leads to a relatively large mass of nonfused macronuclear nodes, generally localized toward the center of the organism (Brasier et al. 2006; Giese 1973; Suzuki 1954; Young 1938), visible in our observation of clustering of macronuclear nodes (Fig. 2C). As no cells visualized in this study formed a uniform single mass, despite tight clustering, we imagine the condensation into a uniform mass prior to elongation is short-lived. After this congregation, the nodes fuse to form a single rod-like macronucleus, which begins stretching throughout much of the cell (Fig. 2D, E; McLoughlin 1957; Suzuki 1954; Young 1938). The elongation of this stage is paralleled with an increase in cell length. The rod-like form is split into distinct macronuclei with the onset of cytokinesis (Fig. 2E; Suzuki 1954; Young 1938). After cytokinesis, the macronucleus reforms its typical "beads-on-a-string" arrangement (Fig. 2A, F).

Macronuclear inclusion

We provide additional data on the nuclear inclusion of *B. americanum*. The macronuclear inclusion of *B. americanum* investigated in this study is approximately 1.9 μm in diameter and tends to be in a DAPI poor region. Young (1938) proposed that this macronuclear inclusion was a protein, perhaps a storage product, used in metabolic activities of macronuclear division. Kennedy (1965) conducted further tests on the inclusion, describing it as a carbohydrate-protein complex, but also suggesting it to be a storage product that the macronucleus could use during division. The macronuclear inclusion existed in the macronuclei in all life cycle stages, inconsistent with Young's hypothesis that it is cyclic in nature and disappears as the cell approaches amitotic division (Young 1938).

Interestingly, the macronuclear inclusion appears to contain blepharismin, the photosensitive pigment found in *Blepharisma* (Fig. 3, 4). The presence of blepharismin in the macronuclear inclusion may either be a natural phenomenon or a fixation artifact. It is possible that blepharismin is chemically attracted to the compound in the inclusion and that the use of Triton-x100 (a chemical detergent) in the fixation of cells could have an effect on its appearance. If, however, the inclusion harboring blepharismin is a natural phenomenon, then its purpose remains unclear, especially considering that studies have found blepharismin to be a photosensitizing pigment involved in transducing perceived light to the photoreceptor system of *B. americanum* (Sobierajska et al. 2006).

Synthesis

We have demonstrated that the heterotrich ciliate *B. americanum* has nearly 1,000 fold as much DNA in its somatic macronucleus as compared to its germline micronucleus (43 ± 8 Gbp compared to 83 ± 16 Mbp respectively). Such high levels of amplification are also documented in the classes Spirotrichea and Phyllopharyngea, two lineages in which extensive fragmentation generates gene-sized chromosomes that are then amplified 1,000 fold or more (Huang and Katz 2014; Xu et al. 2012). In contrast, Karyorelictea—the class sister to the Heterotrichea—are described as paradiploid (e.g. ~2–2.5 N; Raikov and Karadzhan 1985) while other ciliates such as *Tetrahymena* and *Paramecium* amplify their somatic genomes ~45 times and ~800 times, respectively (Duret et al. 2008, Eisen et al. 2006). Hence, ciliates contain a tremendous diversity of nuclear architectures, particularly among somatic macronuclear genomes.

ACKNOWLEDGMENTS

We thank Judith Wopereis for her help and advice with fluorescence microscopy as well as Dr. Jean-David Grattepanche for providing us with the Trizol-based fixative used in this study. This work was supported by both a NIH award (1R15GM113177-01) and a NSF award (DEB-1208741) to LAK.

LITERATURE CITED

Allen, S. E. & Nowacki, M. 2017. Necessity is the mother of invention: ciliates, transposons, and transgenerational inheritance. *Trends Genet.*, 33(3):197–207.

Brasier, M., McLoughlin, N., Green, O. & Wacey, D. 2006. A fresh look at the fossil evidence for early Archaean cellular life. *Philos. Trans. R. Soc. Lond. B Biol. Sci.*, 361:887–902.

Cavalier-Smith, T. 2005. Economy, speed and size matter: evolutionary forces driving nuclear genome miniaturization and expansion. *Ann. Bot.*, 95:147–175.

Cousin, A., Heel, K., Cowling, W. A. & Nelson, M. N. 2009. An efficient high-throughput flow cytometric method for estimating DNA ploidy level in plants. *Cytometry A*, 75A:1015–1019.

Doležel, J., Sgorbati, S. & Lucretti, S. 1992. Comparison of three DNA fluorochromes for flow cytometric estimation of nuclear DNA content in plants. *Physiol. Plant.*, 85:625–631.

Duret, L., Cohen, J., Jubin, C., Dessen, P., Goût, J. F., Mousset, S., Aury, J. M., Jaillon, O., Noël, B., Arnaiz, O., Bétermier, M., Wincker, P., Meyer, E. & Sperling, L. 2008. Analysis of sequence variability in the macronuclear DNA of *Paramecium tetraurelia*: a somatic view of the germline. *Genome Res.*, 18 (4):585–596.

Eisen, J. A., Coyne, R. S., Wu, M., Wu, D. Y., Thiagarajan, M., Wortman, J. R., Badger, J. H., Ren, Q. H., Amedeo, P., Jones, K. M., Tallon, L. J., Delcher, A. L., Salzberg, S. L., Silva, J. C., Haas, B. J., Majoros, W. H., Farzad, M., Carlton, J. M., Smith, R. K., Garg, J., Pearlman, R. E., Karrer, K. M., Sun, L., Manning, G., Elde, N. C., Turkewitz, A. P., Asai, D. J., Wilkes, D. E., Wang, Y. F., Cai, H., Collins, K., Stewart, A., Lee, S. R., Wilamowska, K., Weinberg, Z., Ruzzo, W. L., Wloga, D., Gaertig, J., Frankel, J., Tsao, C. C., Gorovsky, M. A., Keeling, P. J., Waller, R. F., Patron, N. J., Cherry, J. M., Stover, N. A., Krieger, C. J., del Toro, C., Ryder, H. F., Williamson, S. C., Barbeau, R. A., Hamilton, E. P. & Orias, E. 2006. Macronuclear genome sequence of the ciliate Tetrahymena thermophila, a model eukaryote. *PLoS Biol.*, 4:1620–1642.

Giese, A. C. 1973. Blepharisma: the biology of a light-sensitive protozoan. Stanford University Press, Stanford.

Guttes, E. & Guttes, S. 1960. Incorporation of tritium-labeled thymidine into the macronucleus of *Stentor coeruleus*. *Exp. Cell Res.*, 19:626–628.

Huang, J. & Katz, L. A. 2014. Nanochromosome copy number does not correlate with RNA levels though patterns are conserved between strains of the ciliate morphospecies *Chilodonella uncinata*. *Protist*, 165:445–451.

Kaul, S., Koo, H. L., Jenkins, J., Rizzo, M., Rooney, T., Tallon, L. J., Feldblyum, T., Nierman, W., Benito, M. I., Lin, X. Y., Town, C. D., Venter, J. C., Fraser, C. M., Tabata, S., Nakamura, Y., Kaneko, T., Sato, S., Asamizu, E., Kato, T., Kotani, H., Sasamoto, S., Ecker, J. R., Theologis, A., Federspiel, N. A., Palm, C. J., Osborne, B. I., Shinn, P., Conway, A. B., Vysotskaia, V. S., Dewar, K., Conn, L., Lenz, C. A., Kim, C. J., Hansen, N. F., Liu, S. X., Buehler, E., Altafi, H., Sakano, H., Dunn, P., Lam, B., Pham, P. K., Chao, Q., Nguyen, M., Yu, G. X., Chen, H. M., Southwick, A., Lee, J. M., Miranda, M., Toriumi, M. J., Davis, R. W., Wambutt, R., Murphy, G., Dusterhoft, A., Stiekema, W., Pohl, T., Entian, K. D., Terryn, N., Volckaert, G., Salanoubat, M., Choisne, N., Rieger, M., Ansorge, W., Unseld, M., Fartmann, B., Valle, G., Artiguenave, F., Weissenbach, J., Quetier, F., Wilson, R. K., de la Bastide, M., Sekhon, M., Huang, E., Spiegel, L., Gnoj, L., Pepin, K., Murray, J., Johnson, D., Habermann, K., Dedhia, N., Parnell, L., Preston, R., Hillier, L., Chen, E., Marra, M., Martienssen, R., McCombie, W. R., Mayer, K., White, O., Bevan, M., Lemcke, K., Creasy, T. H., Bielke, C., Haas, B., Haase, D., Maiti, R., Rudd, S., Peterson, J., Schoof, H., Frishman, D., Morgenstern, B., Zaccaria, P., Ermolaeva, M., Pertea, M., Quackenbush, J., Volfovsky, N., Wu, D. Y., Lowe, T. M., Salzberg, S. L., Mewes, H. W., Rounsley, S., Bush, D., Subramaniam, S., Levin, I., Norris, S., Schmidt, R., Acarkan, A., Bancroft, I., Quetier, F., Brennicke, A., Eisen, J. A., Bureau, T., Legault, B. A., Le, Q. H., Agrawal, N., Yu, Z., Martienssen, R., Copenhaver, G. P., Luo, S., Pikaard, C. S., Preuss, D., Paulsen, I. T., Sussman, M., Britt, A. B., Selinger, D. A., Pandey, R., Mount, D. W., Chandler, V. L., Jorgensen, R. A., Pikaard, C., Juergens, G., Meyerowitz, E. M., Theologis, A., Dangl, J., Jones, J. D. G., Chen, M., Chory, J., Somerville, M. C. & In, A. G. 2000. Analysis of the genome sequence of the flowering plant *Arabidopsis thaliana*. *Nature*, 408:796–815.

Kennedy, J. R. 1965. The morphology of *Blepharisma undulans* Stein. *J. Protozool.*, 12:542–561.

Kovaleva, V. G., Raikov, I. B. & Miyake, A. 1997a. Fine structure of conjugation of the ciliate *Blepharisma japonicum* 1. Changes of the old macronucleus. *Arch. Protistenk.*, 148:343–350.

Kovaleva, V. G., Raikov, I. B. & Miyake, A. 1997b. Fine structure of conjugation of the ciliate *Blepharisma japonicum* 2. Changes of meiotic and ameiotic micronuclei and development of meiotic and ameiotic macronuclear anlagen. *Arch. Protistenk.*, 148:351–363.

LaJeunesse, T. C., Lambert, G., Andersen, R. A., Coffroth, M. A. & Galbraith, D. W. 2005. *Symbiodinium* (Pyrrhophyta) genome sizes (DNA content) are smallest among dinoflagellates. *J. Phycol.*, 41:880–886.

Liu, Y., Song, X., Gorovsky, M. A. & Karrer, K. M. 2005. Elimination of foreign DNA during somatic differentiation in *Tetrahymena thermophila* shows position effect and is dosage dependent. *Eukaryot. Cell*, 4(2):421–431.

Maurer-Alcalá, X. X. & Katz, L. A. 2016. Nuclear architecture and patterns of molecular evolution are correlated in the ciliate *Chilodonella uncinata*. *Genome Biol. Evol.*, 8:1634–1642.

McGrath, C. L., Zufall, R. A. & Katz, L. A. 2007. Variation in macronuclear genome content of three ciliates with extensive chromosomal fragmentation: a preliminary analysis. *J. Eukaryot. Microbiol.*, 54:242–246.

McLoughlin, D. K. 1957. Macro nuclear morphogenesis during division of *Blepharisma undulans*. *J. Protozool.*, 4:150–153.

Mukherjee, C., Majumder, S. & Lohia, A. 2009. Inter-cellular variation in DNA content of *Entamoeba histolytica* originates from temporal and spatial uncoupling of cytokinesis from the nuclear cycle. *PLoS Negl. Trop Dis.*, 3:e409.

Noirot, M., Barre, P., Louarn, J., Duperray, C. & Hamon, S. 2002. Consequences of stoichiometric error on nuclear DNA content evaluation in *Coffea liberica* var. *dewevrei* using DAPI and propidium iodide. *Ann. Bot.*, 89:385–389.

Ovchinnikova, L., Cheissin, E. & Selivanova, G. 1965. Photometric study of the DNA content in the nuclei of *Spirostomum ambiguum* (Ciliata, Heterotricha). *Acta Protozool.*, 3(7):69–78.

Parfrey, L. W. & Katz, L. A. 2010. Genome dynamics are influenced by food source in *Allogromia laticollaris* strain CSH (Foraminifera). *Genome Biol. Evol.*, 2:678–685.

Postberg, J., Alexandrova, O., Cremer, T. & Lipps, H. J. 2005. Exploiting nuclear duality of ciliates to analyse topological requirements for DNA replication and transcription. *J. Cell Sci.*, 118:3973–3983.

Prescott, D. M. 1994. The DNA of ciliated protozoa. *Microbiol. Rev.*, 58:233–267.

Raikov, I. B. 1996. Nuclei of ciliates. *In:* Haussmann, K. & Bradbury, P. C. (ed.), Ciliates: Cells As Organisms. Gustav Fischer, Stuttgart, p. 221–242.

Raikov, I. B. & Karadzhan, B. P. 1985. Fine structure and cytochemistry of the nuclei of the primitive ciliate *Tracheloraphis crassus* (Karyorelictida). *Protoplasma*, 126(1–2):114–129.

Sobierajska, K., Fabczak, H. & Fabczak, S. 2006. Photosensory transduction in unicellular eukaryotes: a comparison between related ciliates *Blepharisma japonicum* and *Stentor coeruleus* and photoreceptor cells of higher organisms. *J. Photochem. Photobiol., B*, 83:163–171.

Suda, J. & Trávníček, P. 2006. Reliable DNA ploidy determination in dehydrated tissues of vascular plants by DAPI flow cytometry—new prospects for plant research. *Cytometry A*, 69:273–280.

Suzuki, S. 1954. Taxonomic studies on *Blepharisma undulans* Stein with special reference to the macronuclear variation. *J. Sci. Hiroshima Univ.*, 15:205–220.

Turkewitz, A. P., Orias, E. & Kapler, G. 2002. Functional genomics: the coming of age for *Tetrahymena thermophila*. *Trends Genet.*, 18(1):35–40.

Weisz, P. B. 1949. The role of the macronucleus in the differentiation of blepharisma undulans. *J. Morphol.*, 85:503–515.

Weisz, P. B. 1950. Multiconjugation in *Blepharisma*. *Biol. Bull.*, 98:242–246.

Whittaker, K. A., Rignanese, D. R., Olson, R. J. & Rynearson, T. A. 2012. Molecular subdivision of the marine diatom *Thalassiosira rotula* in relation to geographic distribution, genome size, and physiology. *BMC Evol. Biol.*, 12:209.

Xu, K., Doak, T. G., Lipps, H. J., Wang, J. M., Swart, E. C. & Chang, W. J. 2012. Copy number variations of 11 macronuclear chromosomes and their gene expression in *Oxytricha trifallax*. *Gene*, 505:75–80.

Yao, M. & Gorovsky, M. A. 1974. Comparison of sequences of macro-nutrients and micronuclear DNA of *Tetrahymena pyriformis*. *Chromosoma*, 48(1):1–18.

Young, D. 1938. Macronuclear reorganization in *Blepharisma undulans*. *J. Morphol.*, 64:297–353.

Zimin, A., Stevens, K. A., Crepeau, M., Holtz-Morris, A., Koriabine, M., Marcais, G., Puiu, D., Roberts, M., Wegrzyn, J. L., de Jong, P. J., Neale, D. B., Salzberg, S. L., Yorke, J. A. & Langley, C. H. 2014. Sequencing and assembly of the 22-Gb loblolly pine genome. *Genetics*, 196:875–890.

SUPPORTING INFORMATION

Additional Supporting Information may be found online in the supporting information tab for this article:

Table S1. Raw data for cells measured for this study.